Journal of Power Sources 270 (2014) 594–602

Contents lists available at ScienceDirect

Journal of Power Sources

journal homepage: www.elsevier.com/locate/jpowsour

Investigation of a polymer electrolyte membrane fuel cell catalyst layer with bidirectionally-graded composition

Firat C. Cetinbas, Suresh G. Advani, Ajay K. Prasad*

Center for Fuel Cell Research, Department of Mechanical Engineering, University of Delaware, Newark, DE 19716-3140, USA

HIGHLIGHTS

- Improved agglomerate model is used to study the PEM fuel cell catalyst layer.
- Catalyst and ionomer loadings varied in through-thickness and in-plane directions.
- Higher catalyst, ionomer loading at membrane/CL interface improves performance.
- Bidirectionally-graded CLs are investigated for the first time.
- Bidirectional grading improves performance in ohmic and mass transport regimes.

ARTICLE INFO

Article history:
Received 16 May 2014
Received in revised form
21 July 2014
Accepted 22 July 2014
Available online 30 July 2014

Keywords:
Functionally-graded catalyst layer
Pt loading
Nafion loading
Ohmic loss
Mass transport loss
Bidirectional grading

ABSTRACT

The catalyst layer (CL) of the polymer electrolyte membrane (PEM) fuel cell must be modeled accurately in order to resolve the effects of complex interactions between charge and mass transport on the fuel cell's electrochemical reactions. In previous work, we developed an agglomerate model [1] which correctly accounts for variations in the agglomerate surface area as the CL constituents are varied to provide a better estimate of diffusion losses. Here, this improved agglomerate model is employed to investigate a PEM fuel cell catalyst layer with a functionally-graded composition. We present results for varying catalyst and ionomer loadings in both the through-thickness and in-plane directions. In agreement with experimental observations, we find that a higher catalyst and/or ionomer loading at the membrane/CL interface improves performance especially in the ohmic loss regime. Similarly, improved performance is observed for higher catalyst and/or ionomer loadings under the channel in the mass transport loss regime. In addition, we investigated bidirectionally graded CLs for the first time. It is observed that higher performance can be obtained with bidirectionally graded CLs in both ohmic and mass transport loss regimes.

1. Introduction

Over the past two decades, many important developments have brought PEM fuel cells closer to commercialization. Although substantial experimental and computational research has been conducted on all aspects of PEM fuel cells, the sluggish reactions in the cathode catalyst layer (CL) remain a major limiter of performance. Because all of the fuel cell's electrochemical reactions and significant charge and mass transport occur within the catalyst layer, the overall accuracy of fuel cell computational models depends critically on an accurate representation of the catalyst layer. Therefore, modeling and simulation of the CL continues to attract significant research effort.

The CL is a 10–30 μm thick composite structure containing platinum (Pt), carbon support, ionomer electrolyte, gas pores, and liquid water. Within this structure, reactions are catalyzed by Pt while the carbon support and ionomer phase conduct electrons and protons, respectively, and the pores create pathways for reactant gas access and product removal. Consequently, the CL activity consists of multiple competing transport processes which require an optimum loading of catalyst, carbon support, and ionomer distributed within a layer of adequate porosity. For example, whereas a higher Pt loading would improve the reaction rate, it would adversely impact reactant transport due to decreased porosity. Similarly, a higher volume fraction of ionomer would improve proton transport, but also at the cost of reduced reactant

* Corresponding author.
E-mail address: prasad@udel.edu (A.K. Prasad).

http://dx.doi.org/10.1016/j.jpowsour.2014.07.148
0378-7753/

transport due to a lower porosity. In this context, several experimental studies [2–5] have been performed to optimize the CL composition to improve the overall PEM fuel cell efficiency.

Uchida et al. [2] experimentally studied the effects of ionomer loading and reported an optimum value for ionomer loading that gave better performance over the entire operating regime. Similarly, Antolini et al. [3] reported an optimum Nafion loading which minimizes activation and ohmic losses. Paganin et al. [4] examined both platinum-to-carbon weight ratio (%Pt|C) and Nafion loading and also reported optimum values for these quantities. Passalacqua et al. [5] unified the optimum Nafion loading results of [2–4] by defining a parameter called NFP (Nafion percentage). They also performed experiments and reported an optimum NFP value of 33% which agrees with the optimum NFP loading of about 33–40% given by Refs. [2–4]. Qi and Kaufman [6] studied the effects of Pt loading and %Pt|C for a CL with 33% NFP which was the optimal Nafion loading according to their experimental data. They reported optimum Pt loadings for 20% and 40% Pt|C ratios.

The literature contains many other experimental studies that focus on the optimization of the CL composition. However, most of these consider a spatially-uniform CL composition. There are relatively few experimental attempts [7–11] to investigate functionally-graded CL compositions. Ticianelli et al, Antoine et al, [7–9] studied the effect of a graded catalyst loading through the thickness of the CL. Ticinalli et al. [7,8] reported performance improvement when the catalyst concentration was increased at the membrane/CL interface. Antoine et al. [9] investigated porous and non-porous active layers. For the porous case, they observed performance improvement when the catalyst loading was increased adjacent to the membrane. On the other hand, they reported better performance when the catalyst loading was higher at the gas diffusion layer (GDL)/CL interface for the non-porous electrode. Wilkinson and Pierre [10] studied graded catalyst loading along the length of the gas channel and reported enhanced performance when the catalyst loading was higher towards the inlet. In addition, Xie et al. [11] examined the effect of an NFP gradient through the thickness of the CL and reported improved performance for a higher NFP towards the membrane/CL interface.

Determining an optimal CL composition requires a good understanding of the physical phenomena occurring within the CL. Numerical models serve as a valuable tool to provide detailed insight that might be difficult to observe experimentally. The literature contains several numerical studies [12–17] that have investigated functionally-graded CL compositions. Wang et al. [12] developed a 1D cathode model based on percolation theory that characterizes effective CL properties and the active reaction area. Employing a macro-homogeneous model for the CL, they investigated the effects of graded NFP through the CL thickness. In agreement with experimental results [11], they reported better performance for high NFP close to the membrane/CL interface. However, their use of the macro-homogeneous approach to model the CL prevented them from predicting the effects of the graded CL in the mass transport regime. Using the classical agglomerate approach, Sun et al. [13] reported improved performance for higher Nafion loading towards the membrane with their 2D cathode model. Song et al. [14] optimized the Pt and NFP distributions through the thickness of the CL with their 1D cathode model which employs a macro-homogeneous approach by considering the effect of liquid water saturation. They obtained the optimum NFP distribution as a linearly increasing function from the membrane to the GDL. For the optimum Pt loading distribution, they obtained a convex increasing function from the membrane to the GDL.

Schwarz and Djilali [15] developed a multiple thin-film agglomerate model to account for the effect of liquid water in the CL. With their improved agglomerate approach they investigated graded catalyst loading cases in three separate directions with a 3D fuel cell model. They reported improved performance when the catalyst loading was higher towards the channel inlet, and when it was higher towards the channel in the lateral in-plane direction. Srinivasarao et al. [16] investigated the graded CL composition in the through-thickness direction by considering multiple stacked CLs within their 2D cathode model. They used the multiple thin-film agglomerate model as in Ref. [15] and investigated graded catalyst, NFP and Pt|C distributions separately. In addition, Mukherjee and Wang [17] studied a bi-layer CL with direct numerical simulation. In agreement with the previous studies they also reported increased performance when the Nafion loading was higher towards the membrane/CL interface.

It should be noted that the fidelity of PEM fuel cell simulations depends critically on the employed CL modeling approach. The agglomerate approach is the most comprehensive among the various CL models which are reviewed in detail in Ref. [18]. Recently, the agglomerate model was modified by employing discrete catalyst particles [18,19] in order to more accurately predict the effect of catalyst loading. In addition, in Ref. [1], we presented an improved agglomerate model incorporating a sphere-packing approach to physically model the effect of porosity on the effective surface area of agglomerates (which was ignored in the previous approaches) as this is a crucial parameter to determine diffusion losses. It was shown in Ref. [1] that the new agglomerate model's predictions were physically realistic and gave good agreement with experimentally observed trends.

In this study, we employed the model in Ref. [1] to investigate the effects of graded CL compositions. In-plane, through-thickness, and bidirectionally-graded CLs were studied as depicted schematically in Fig. 1. It should be noted that the effect of CL porosity on surface area, which is captured in Ref. [1], was not accounted for in previous agglomerate models [13,15,16] while investigating the graded CL composition. Moreover, none of the previous studies provided guidelines for the range of variation in loading within the graded CL. Most importantly, the multidirectionally-graded CL composition as shown in Fig. 1c) has not been studied to date.

2. Model description

The complete 2D, steady-state cathode model is explained in detail in Ref. [1]. The model accounts for the transport of chemical species, electrons, and ions in the GDL and the CL under the assumption of an isothermal, isobaric, and steady-state process. The computational domain encompasses half of the channel and half of the land area as shown in Fig. 2. The associated geometric parameters are listed in Table 1.

The governing equations for species and charge transport are [1]:

$$\nabla\cdot\left[-\rho\omega_j\sum_k D_{jk}^{\mathrm{eff}}\nabla\frac{\omega_k}{M_k}M_n\right]=R_j \tag{1}$$

$$\nabla\cdot\left(\sigma_m^{\mathrm{eff}}\nabla\varnothing_m\right)=\nabla\cdot i \tag{2}$$

$$\nabla\cdot\left(\sigma_s^{\mathrm{eff}}\nabla\varnothing_s\right)=-\nabla\cdot i \tag{3}$$

where ρ is the mixture density, ω_j is the mass fraction, D_{jk}^{eff} is the effective diffusivity, M_i is the molecular weight, R_j is the source term calculated from the electrochemical reactions, σ_m^{eff} is the effective ionic conductivity, $\varnothing_m$ is the ionic potential, σ_s^{eff} is the electronic conductivity, $\varnothing_s$ is the electric potential, and $\nabla\cdot i$ is the current generation due to the electrochemical activity in the CL [1].

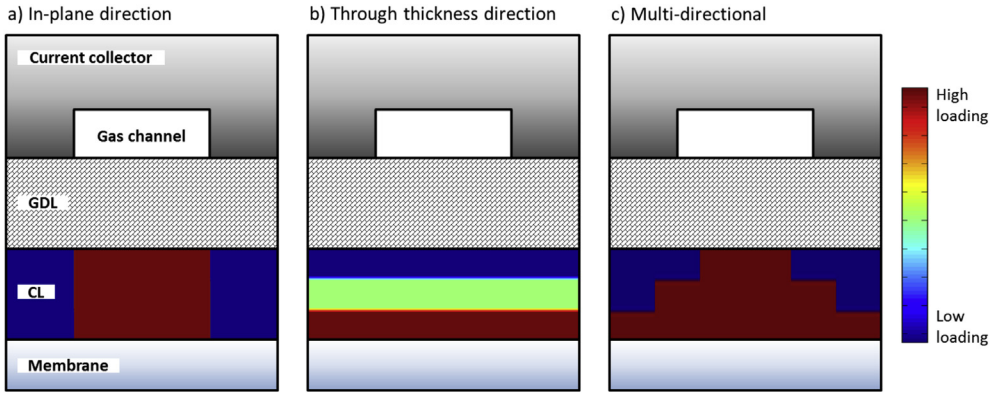

Fig. 1. Schematic representation of graded CL composition in various directions.

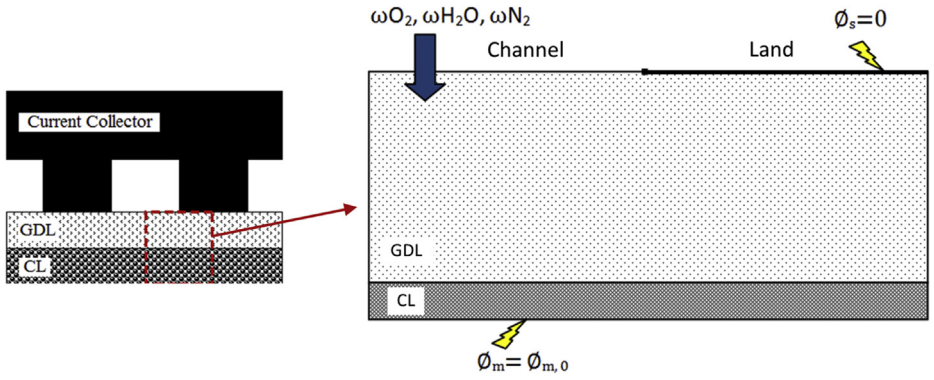

Fig. 2. 2D computational domain with half-cell section view [1].

The CL is modeled by employing the spherical agglomerate approach. As described in Ref. [1] the sphere-packing approach was used to provide as accurate estimate of the effective surface area as the agglomerates begin to overlap with decreasing porosity. The classical agglomerate equations were rearranged with the assumption that the reactant concentration at the agglomerate surface does not change between a single and an overlapping agglomerate. Then the reaction rate is calculated based on the reactant flux at the agglomerate surface using the following equations [1]:

$$\nabla \cdot i = I_v^{CL} = -4FD\frac{(C_0 - C_s)}{\delta}\left(\frac{r_{agg}}{r_{agg}+\delta}\right)a_{agg} \tag{4}$$

$$C_s = \frac{C_0}{1 + \frac{D_{agg}}{D}\left(\frac{\delta}{r_{agg}+\delta}\right)\left(\coth(Th)Th - 1\right)} \tag{5}$$

$$C_0 = \frac{P_{O_2}}{H} \tag{6}$$

where F is the Faraday constant, D is the diffusivity of oxygen in the ionomer, C_0 is the oxygen concentration at the ionomer film surface, C_s is the oxygen concentration at the agglomerate core surface, r_{agg} is the agglomerate radius, δ is the ionomer film thickness, a_{agg} is the effective surface area, D_{agg} is the effective diffusivity in the agglomerate core, Th is the Thiele modulus, and H is Henry's constant.

Table 1
Geometric parameters for the 2D computational domain.

Channel width	w_{ch}	1.5 mm
Land width	w_l	1.5 mm
GDL thickness	t_{GDL}	250 μm
CL thickness	t_{CL}	15 μm

As the porosity is decreased, adjacent agglomerates begin to touch and then overlap which reduces the available agglomerate surface area. The effective surface area reduction due to decreasing porosity is modeled using the sphere-packing approach and calculated as [1]:

$$a_{agg} = 4\pi n(r_{agg}+\delta)^2 \quad \text{for } \varepsilon_v \geq \varepsilon_{v,cr} \tag{7}$$

$$a_{agg} = \frac{\pi}{\alpha_m D_p (1-f)^2}\left[1 - \frac{mf}{2}\right] \quad \text{for } \varepsilon_{v,o} \leq \varepsilon_v < \varepsilon_{v,cr} \tag{8}$$

$$a_{agg} = f(\varepsilon_v) = \left(\frac{f'(\varepsilon_{v,o})\varepsilon_{v,o} - f(\varepsilon_{v,o})}{\varepsilon_{v,o}^2}\right)\varepsilon_v^2 + \left(\frac{2f(\varepsilon_{v,o}) - f'(\varepsilon_{v,o})\varepsilon_{v,o}}{\varepsilon_{v,o}}\right)\varepsilon_v \quad \text{for } \varepsilon_v < \varepsilon_{v,o} \tag{9}$$

where n is the number of agglomerates per unit volume of the CL, ε_v is CL porosity, $\varepsilon_{v,cr}$ is the critical porosity, $\varepsilon_{v,o}$ is the limiting porosity, D_p is the agglomerate diameter, f is the overlapping ratio, m is the number of contact points, and α_m is the packing factor [1]. Here it is important to note that the catalyst ink composition is specified in terms of the weight fractions of its various components which are expressed in terms of the Pt loading to calculate the porosity as in

Ref. [1]. The α_m and m values employed in the current simulations correspond to the rhombohedral packing scheme. One can refer to [1] for additional information.

The boundary conditions for the governing equations can be written by referring to Fig. 2 as follows. For species transport (Maxwell-Stefan equation), the inlet mass fractions are specified at the channel and the no-flux condition is assigned to all the remaining boundaries. For electron transport, the electric potential is set to zero at the land, while the no-flux condition is assigned to all the remaining boundaries. For ionic charge conservation, the ionic potential is set to $\varnothing_{m,0}$ at the membrane/CL interface and all the other boundaries are defined as no-flux. The parameters for the baseline case are listed in Table 2.

3. Results and discussion

In Ref. [1] we studied the effect of CL composition on performance using our new sphere-packing approach to determine the effective agglomerate surface area which is required to accurately calculate the diffusion losses. The model was validated in Ref. [1] by comparing the predicted polarization curve against experimental data. It was also shown that the predicted current distribution matched the results from previously published numerical studies. In addition, the model's predictions for the effect of NFP on current density at a constant operating voltage was shown to agree with experimental data. All of the results in Ref. [1] pertained to spatially-uniform CL compositions. Here, we employ the model of [1] to investigate the effect of graded CL composition on performance.

It is evident that the concentration and transport of reacting species (ions, electrons, O_2) in the CL is not spatially uniform either in the through-thickness or in-plane directions. For instance, the proton flux is the highest at the membrane/CL interface and drops to zero at the GDL/CL interface. Similarly, the reactant flux is highest at the GDL/CL interface and drops to zero at the membrane/CL interface. Consequently, the reaction rate is also not spatially uniform within the CL. These observations suggest that more efficient reactions and higher catalyst utilization could be achieved by functionally grading the CL composition to fit the requirements imposed by these non-uniform reaction rates. Increasing the effectiveness of the CL by grading its composition requires a good understanding of the effects of the charge and species transport mechanisms on the reaction rate. In addition, the reaction rate distribution and the overpotential in the CL are highly dependent on the operating regime.

O_2 mass fraction distributions for activation (nominal cathode overpotential (NCO) = 0.2 V), ohmic (NCO = 0.5 V), and mass transport (NCO = 0.9 V) regimes are shown in Fig. 3 for the spatially-uniform CL composition case. In the activation regime, the O_2 concentration throughout the CL is high and uniform as the O_2 consumption rate is small compared to the rate of diffusion (Fig. 3a)). In contrast, the reaction rate greatly exceeds the rate of diffusion in the mass transport regime due to which the under-land region experiences greatly reduced O_2 concentrations (Fig. 3c)).

Table 2
Parameter values used in the cathode simulation for the baseline case.

Pressure	P	2.04 atm (30 psi)
Temperature	T	353 K
Relative humidity	RH	0.7
Platinum loading	m_{Pt}	0.003 kg m^{-2}
Pt to C weight ratio	Pt|C	0.2
Ionomer weight fraction	NFP	0.30
Agglomerate radius	r_{agg}	$3E{-}6$ m
Ionomer film thickness	δ	$145E{-}9$ m
Henry's constant	H	31663 Pa m^3 mol^{-1}
Reference exchange current density	$i_{0,ref}$	0.00105 A m^{-2} for $V_c \geq 0.8$ V 0.06948 A m^{-2} for $V_c \leq 0.8$ V
Cathode charge transfer coefficient	α_c	1 for $V_c \geq 0.8$ V 0.61 for $V_c \leq 0.8$ V
Electron conductivity	σ_s	150 S m^{-1}
Diffusivities	D_{O_2,N_2}	$1.86E{-}5$ m^2 s^{-1}
	D_{H_2O,N_2}	$2.58E{-}5$ m^2 s^{-1}
	D_{O_2,H_2O}	$2.47E{-}5$ m^2 s^{-1}

The overpotential is the difference between electron and ionic potentials. It conveys information about the effects of both the electron and ion transport. Fig. 4 illustrates the overpotential distribution in the CL for activation (NCO = 0.2 V), ohmic (NCO = 0.5 V), and mass transport (NCO = 0.9 V) regimes. The overall trend in Fig. 4 indicates that the overpotentials are always higher under the land (due to shorter electron paths) and close to the membrane/CL interface (due to higher ion concentrations). In the activation regime, the spatial differences in overpotential are very small; the overpotential is slightly higher under the land than under the channel due to shorter electron paths. Furthermore, the electrolyte potential only varies in the through-thickness direction in the activation regime as can be seen in Fig. 5a). In the ohmic loss region, the spatial variations in overpotential become greater mainly due to a higher ionic potential drop as illustrated in Fig. 5b). Fig. 5b) indicates that the ionic potential greatly decreases under the channel due to an abundance of reactant which results in higher ion consumption under the channel. In the mass transport regime, the overpotential distribution in Fig. 4c) closely follows the ionic potential distribution Fig. 5c) which shows that ions cannot be consumed under the land at high reaction rates due to a lack of reactant.

The reaction rate distribution for the spatially-uniform CL composition is shown in Fig. 6 for the same three operating regimes. The location of the highest reaction rate can be explained by combining the effects of mass and charge transport presented in Figs. 3–5. The reaction rate distribution in Fig. 6a) is almost identical to the overpotential distribution in Fig. 4a) which implies that the reactions are dominated by local overpotentials in the activation region as the reactant concentration is almost uniform throughout the CL. In the ohmic loss regime, the highest reaction rate is observed at the junction of the land and the channel at the membrane/CL interface (Fig. 6b)). Thus, it can be inferred that the ohmic loss region is almost equally dominated by both reactant and charge transport such that the highest reaction rate is obtained where all species can be transported easily. When the reaction rate increases further, reactant transport begins to dominate and the highest reaction rate is obtained under the channel (Fig. 6c)). In Fig. 6c), it is also observed that the reaction rate changes only in the in-plane direction under the land due to severe reactant starvation there. Furthermore, close to the GDL/CL interface in Fig. 6, higher reaction rates are observed at the channel/land junction which can be attributed to shorter electron paths.

It is important to note that the highest reaction rates are always obtained at the membrane/CL interface showing the importance of ion concentration on reactions. This observation suggests that the CL composition could be graded to improve ion transport. Accordingly, we first investigate the case with graded NFP in the through-thickness direction while fixing the total Nafion content. The CL is divided into three layers of equal thickness, each with a different NFP, but with a constant average NFP of 30%. The resulting performance curves are presented in Fig. 7.

Fig. 7 indicates that the performance is significantly affected by the NFP gradient in through-thickness direction. A higher NFP close to the membrane results in improved performance as was experimentally observed in Ref. [11]. Most of the improvement is observed in the ohmic loss region because higher NFP close to the membrane improves the transport of ions migrating into the CL

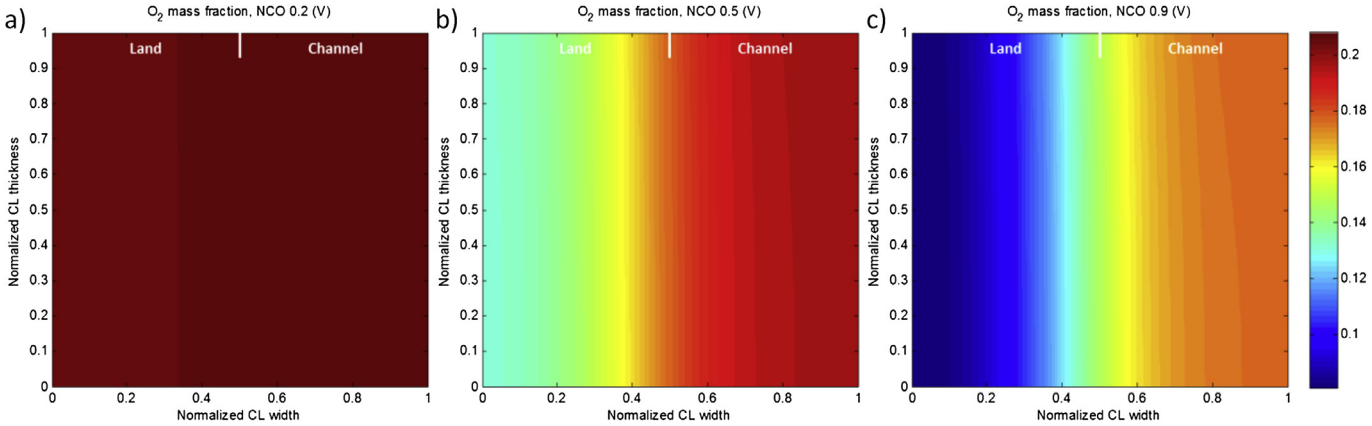

Fig. 3. O_2 mass fraction distributions in the CL for different operating regimes (spatially-uniform CL composition).

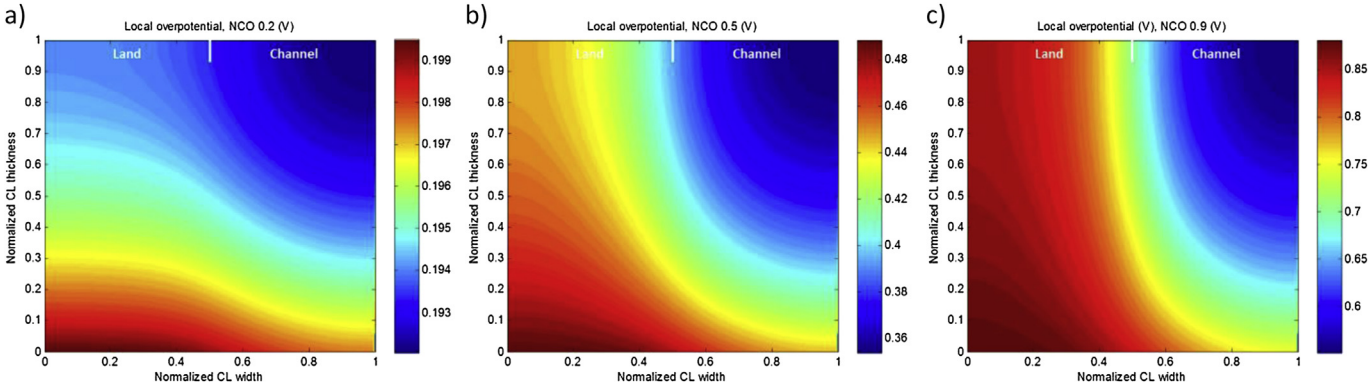

Fig. 4. Absolute values of overpotential (V) distribution in the CL for different operating regimes (spatially-uniform CL composition).

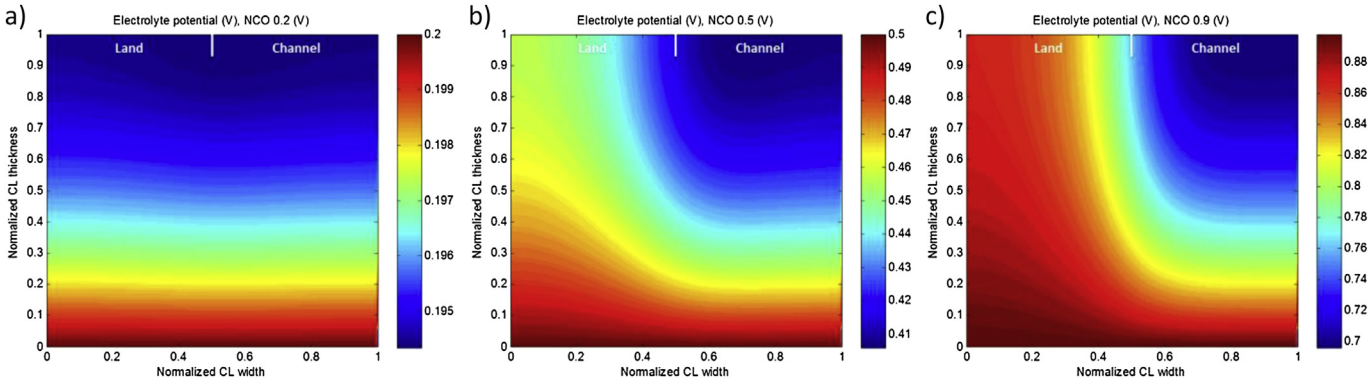

Fig. 5. Ionic potential (V) distribution in the CL for different operating regimes (spatially-uniform CL composition).

from the membrane. In addition, decreasing NFP close to the GDL improves reactant transport by increasing the porosity. Due to these effects, the maximum power density is improved by about 7% over the baseline case. On the other hand, if we increase the NFP content close to the GDL and decrease the NFP close to the membrane, both the ion and reactant transport are negatively affected, and hence the performance decreases as seen in Fig. 7. Furthermore, Fig. 7 shows that the NFP close to the membrane should not be increased beyond about 40% due to diffusion limitations. In other words, there is an optimal NFP gradient in the through-thickness direction. In Fig. 7 it is observed that diffusion losses first decrease the current generation only in the mass transport region for the high NFP gradient configuration of 0.45_0.30_0.15, whereas they affect the entire polarization curve for the 0.50_0.30_0.10 NFP configuration.

Next, we investigated the graded catalyst loading in through-thickness direction. Similar to the NFP gradient case, the CL is divided into three layers of equal thickness, each with a different catalyst loading, but with a constant average loading of 0.30 mg cm^{-2}. The resulting performance curves in Fig. 8 indicate that concentrating the catalyst towards the membrane (the ion-enriched region in the CL) increases Pt utilization and improves performance in agreement with the experimental observations of [7–9]. The maximum power density is improved by about 3.2% over

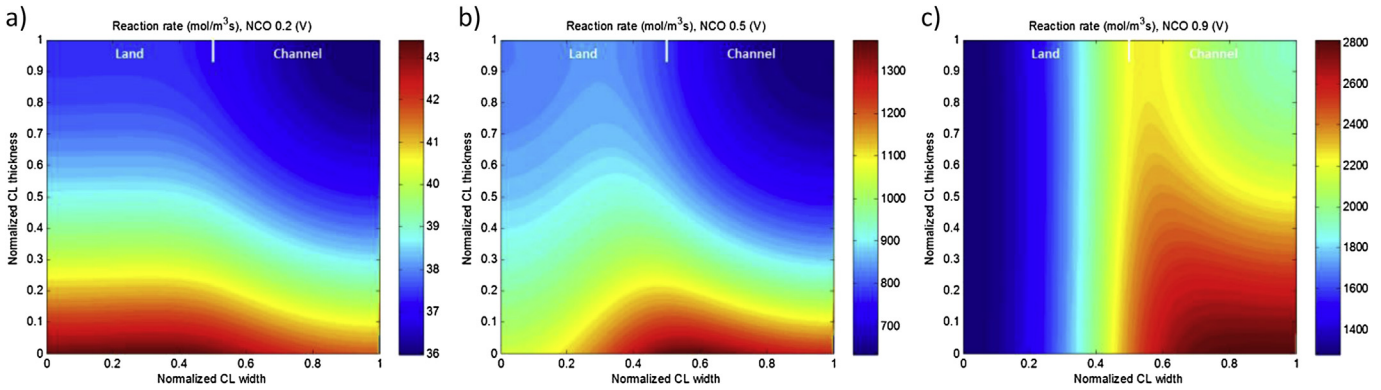

Fig. 6. Reaction rate (mol m^{-3} s) distribution in the CL for different operating regimes (spatially-uniform CL composition).

the baseline case. In contrast, biasing the catalyst concentration towards the GDL lowers the performance as well as catalyst utilization as the reaction rates are always lower at the GDL/CL interface. Attempting to improve Pt utilization by further concentrating catalyst at the membrane/CL interface is not feasible because excessive catalyst loading can block the pores and reduce reactant access leading to diffusion losses as observed in Fig. 8.

We also studied the effect of graded Pt|C weight ratio in the through-thickness direction while fixing the Pt loading, NFP and overall Pt|C ratio. The resulting polarization curves are illustrated in Fig. 9. It is important to note that, for the same NFP and Pt loading, a higher Pt|C weight ratio implies lower Nafion and carbon loadings which result in higher porosity. Hence, higher Pt|C would improve reactant transport, whereas lower Pt|C would benefit the ohmic region. Fig. 9 shows that a lower Pt|C close to the membrane improves performance in agreement with our previous findings because a lower Pt|C corresponds to a higher Nafion loading which improves ion transport. Concurrently, a higher Pt|C close to the GDL enhances porosity and improves diffusion. The maximum power density is improved by about 12% over baseline for the 0.15_0.25_0.35 Pt|C configuration. This performance improvement is higher than that seen in Fig. 7 due to the combined effects of highly improved reactant transport (higher porosity) close to the GDL and higher Nafion loading close to the membrane. On the other hand, the inverse configuration lowers performance as shown in Fig. 9.

In addition, we studied the case for varying Pt|C ratio but with fixed Pt and Nafion loadings. In this case, varying Pt|C only changes the carbon loading and the porosity. The performance curves in Fig. 10 indicate that the diffusion loss region is improved for both configurations. It should be noted that the average porosity decreases for both configurations from 0.55 to around 0.5 which increases the effective surface area and improves performance in the diffusion loss region. The ohmic loss region is not noticeably improved for either configuration as the electron potential drop in the through-thickness direction is insignificant. Fig. 10 indicates that a greater performance improvement is observed for the configuration with higher Pt|C ratio close to the GDL; higher Pt|C close to the GDL provides more pathways for reactant access to the active area and improves mass transport.

Another important observation from Figs. 3–6 is that the reaction rates are always higher under the channel than under the land in the mass transport regime. This suggests that the CL composition could be functionally graded in the in-plane direction to improve reactant transport.

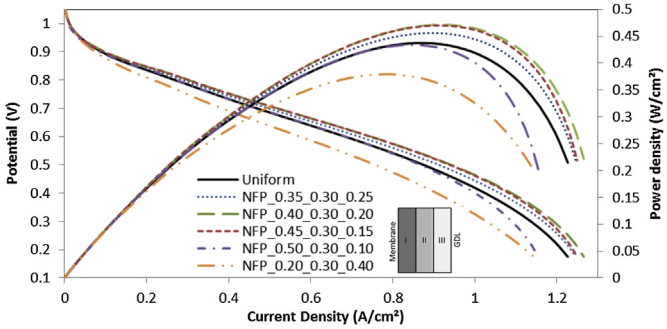

Fig. 7. Effect of NFP grading in the through-thickness direction on cathode performance; the average NFP is fixed at 30%.

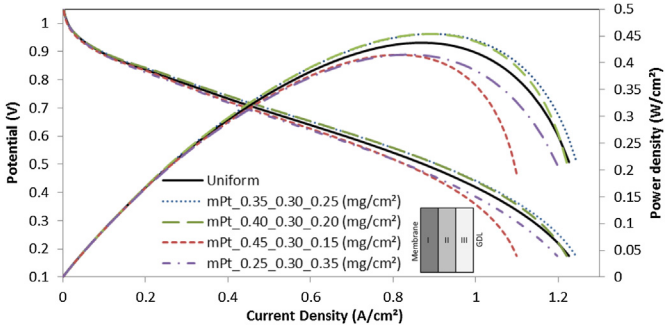

Fig. 8. Effect of catalyst grading in the through-thickness direction on cathode performance; the average catalyst loading is fixed at 0.30 mg cm^{-2}.

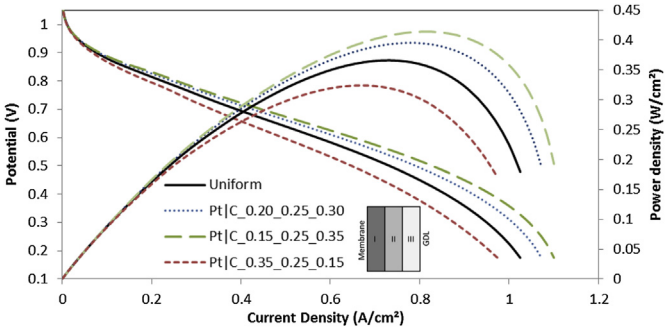

Fig. 9. Effect of Pt|C grading in the through-thickness direction on cathode performance for constant catalyst loading and NFP. The average Pt|C is fixed at 0.25.

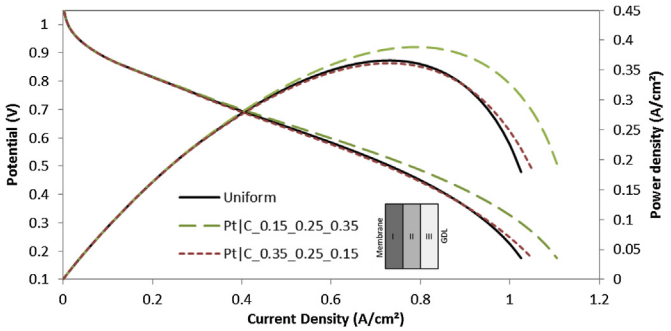

Fig. 10. Effect of Pt|C grading in the through-thickness direction on cathode performance for constant catalyst and Nafion loadings (m_{Pt} = 0.3 mg cm^{-2}, m_N = 0.514 mg cm^{-2}). The average Pt|C is fixed at 0.25.

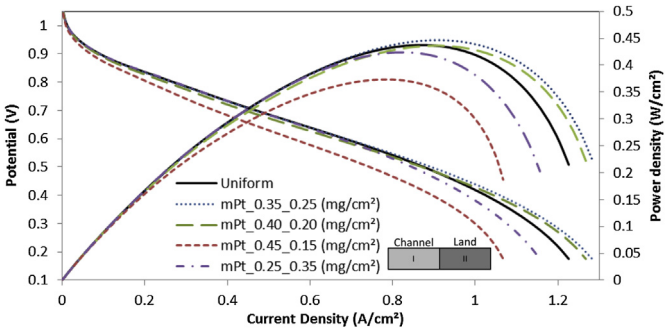

Fig. 12. Effect of catalyst grading in the in-plane direction on cathode performance; the average catalyst loading is fixed at 0.30 mg cm^{-2}.

We investigate this idea by first grading the NFP in the in-plane direction while fixing the average NFP in the CL at 30%. We consider the case where the CL is divided into two parts (under-channel and under-land) each with different NFP values. The resulting polarization curves in Fig. 11 show that higher NFP under the channel improves performance in the diffusion-loss region. Increasing the under-channel NFP improves ion conductivity in the through-thickness direction leading to higher ion transport towards the GDL interface under the channel where the reactant concentration is high enough to consume these ions. Increasing the under-channel NFP improves the power density by about 6.5% over baseline. In contrast, increasing the NFP under the land results in poor performance especially in the diffusion loss region because the under-land region suffers from insufficient O_2 concentration to consume the ions. Fig. 11 also indicates that increasing the under-channel NFP beyond about 40% exacerbates diffusion losses. The effect of decreased porosity is first felt only in the diffusion loss region for NFP_0.45_0.15 configuration; further NFP grading causes diffusion losses throughout the polarization curve as see for the NFP_0.50_0.10 configuration.

Next, we examine the effect of catalyst grading in the in-plane direction to improve reactant transport in the mass transport regime. Similar to the laterally-graded NFP case, we divided the CL into under-channel and under-land regions, each with a different catalyst loading. The effect of in-plane catalyst gradient on performance in Fig. 12 shows that concentrating the catalyst under the channel improves performance in the diffusion-loss region. The improvement can be attributed to increased catalyst utilization because the under-channel region is enriched with reactant compared to the under-land region especially in the mass transport regime. The maximum power density is increased about 2.5% over baseline by concentrating the catalyst under the channel. Similar to previous results, there is an optimum gradient for the Pt loading due to diffusion limitations.

Next, we study the effect of Pt|C grading in the in-plane direction while keeping the Pt loading and NFP content constant in the CL. Again, the under-land and under-channel regions of the CL are loaded with different Pt|C ratios. The resulting polarization curves presented in Fig. 13 indicate that a lower Pt|C ratio under the channel improves performance especially in the diffusion-loss region. The performance improvement in Fig. 13 can be attributed to higher Nafion and carbon loadings under the channel corresponding to a lower Pt|C ratio; then, improved ion conduction under the channel increases performance. The maximum power density is improved about 9.5% over baseline as shown in Fig. 13. Although Fig. 13 reveals the same trends as in Fig. 11, the former yields higher performance improvement due to better reactant transport under higher porosity. As expected, the inverse configuration results in lower current densities in the mass transport regime.

In Fig. 13 the effect of graded Pt|C is dominated by the effect of Nafion loading (similar to the case in Fig. 11) which varies due to the constant NFP assumption. Therefore, we next isolate the effect of laterally grading the carbon loading by varying the Pt|C ratio at a fixed Nafion loading. The resulting performance curves presented in Fig. 14 show that the configuration with higher Pt|C under the land does not experience a noticeable mass transport loss due to a locally lower carbon loading and higher porosity. Hence, such a Pt|C grading improves reactant transport under the land which typically suffers from diffusion losses at high reaction rates. In contrast, the inverse case of lower Pt|C under the land reveals a distinct mass transport loss region. However, the case of lower Pt|C under the land performs slightly better in the ohmic loss region as the effective under-land surface area is increased over the baseline

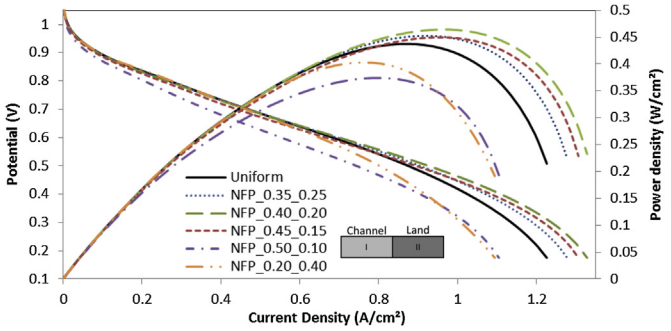

Fig. 11. Effect of NFP grading in the in-plane direction on cathode performance; the average NFP is fixed at 30%.

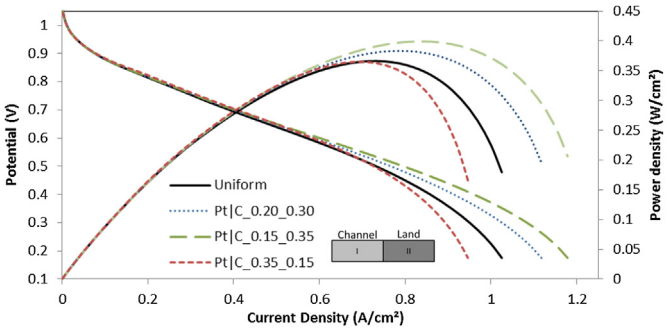

Fig. 13. Effect of Pt|C grading in the in-plane direction on cathode performance for constant catalyst loading and NFP. The average Pt|C is fixed at 0.25.

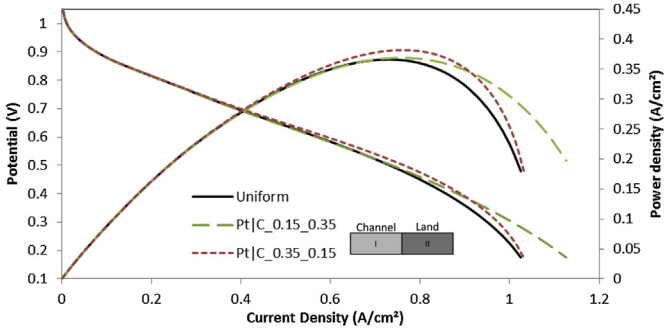

Fig. 14. Effect of Pt|C grading in the in-plane direction on cathode performance for constant catalyst and Nafion loadings (m_{Pt} = 0.3 mg cm^{-2}, m_N = 0.514 mg cm^{-2}). The average Pt|C is fixed at 0.25.

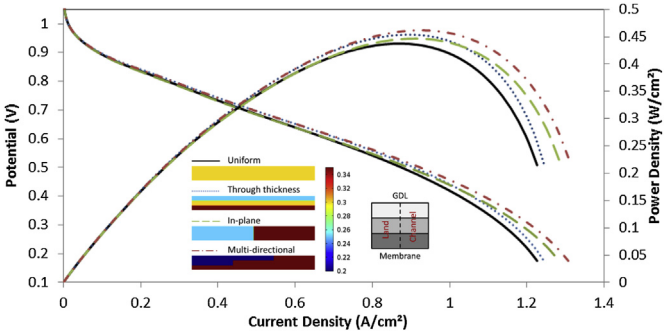

Fig. 16. Effect of bidirectional catalyst grading on performance; the average catalyst loading is fixed at 0.30 mg cm^{-2}.

case. Higher effective surface area under the land increases current generation in the ohmic loss regime leading to higher reaction rates under the land as illustrated in Fig. 6b). Due to this improvement in the ohmic loss region, the maximum power density is increased by about 4% over baseline.

So far, we studied the effects of graded CL composition in the through-thickness and in-plane directions separately. Graded composition in the through-thickness direction mainly improves performance in the ohmic loss regime by improving ion transport. Graded CL composition in the in-plane direction mainly improves performance in the mass transport regime by improving reactant transport. It is worthwhile to investigate if grading the CL composition in both directions simultaneously can provide a performance that exceeds the benefits of CL grading solely in either individual direction.

Accordingly, we first examined the benefit of grading NFP in the through-thickness direction, the in-plane direction, and bidirectionally as illustrated in Fig. 15 while keeping the average NFP constant at 30%. Fig. 15 indicates that grading the NFP bidirectionally improves performance both in the ohmic and mass transport loss regimes. Bidirectional grading improves ion transport in the through-thickness direction concentrating Nafion close to the membrane. At the same time, concentrating Nafion under the channel improves ion transport and reactant consumption in the mass transport regime for which the reactant is abundant only under the channel.

Finally, we compare the performance obtained by grading the catalyst in the through-thickness direction, the in-plane direction, and bidirectionally as illustrated in Fig. 16 while keeping the average catalyst loading constant at 0.30 mg cm^{-2}. As expected, the bidirectional grading superposes the positive effects of the through-thickness and in-plane cases. Therefore, bidirectionally-graded catalyst loading provides improved performance in both ohmic and diffusion-loss regions.

Figs. 15 and 16 indicate that bidirectional grading would be a desirable option if such a CL could be manufactured. In this study, we have only considered one out of several possible multi-directional grading configurations. The results are promising, and suggest that performance could be improved further by simultaneously optimizing the CL composition gradients along multiple directions. Further study is required to optimize the CL topology for superior performance over a range of operating conditions.

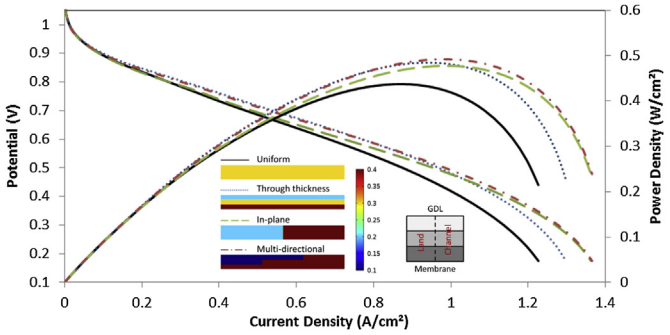

Fig. 15. Effect of bidirectional NFP grading on performance; the average NFP is fixed at 30%.

4. Summary and conclusions

In this study, we examined functionally-graded catalyst layer compositions by employing our two-dimensional cathode model which incorporates an improved agglomerate approach [1] to accurately model diffusion limitations. First, the effects of charge and mass transport mechanisms on reaction rate distribution were investigated for different operating regimes. It was observed that the highest reaction rates are always obtained at the membrane/CL interface for all operating regimes due to higher local ion concentrations. In addition, higher reaction rates were observed under the channel in the mass transport regime due to the greater abundance of reactant.

Based on these observations, we studied graded CL compositions to improve ion and reactant transport in the CL. A higher NFP close to the membrane improves ion transport and performance in the ohmic loss region. Higher NFP under the channel improves performance in the mass transport region due to both improved ion and reactant transport. Concentrating Pt close to the membrane improves performance by increasing catalyst utilization in this ion-rich region. In addition, higher catalyst loading under the channel improves performance in the mass transport regime in this reactant-rich region. Optimum gradients were found for both NFP and catalyst loading. Increasing the gradient beyond a critical value results in decreased performance due to diffusion limitations.

We also studied bidirectionally-graded CL compositions for the first time. Bidirectional grading yields superior performance over unidirectional grading due to simultaneous improvements in both the ohmic loss and mass transport regimes.

Acknowledgments

This work was conducted under the University of Delaware's Fuel Cell Bus Program to research, build, and demonstrate fuel cell powered hybrid vehicles for transit applications. This program is

funded by the Federal Transit Administration at the Center for Fuel Cell Research at the University of Delaware.

Nomenclature

a_{agg}	effective surface area in CL $m^2\ m^{-3}$
C_0	ionomer film surface oxygen concentration mol m^{-3}
C_s	agglomerate surface oxygen concentration mol m^{-3}
$D_{i,j}$	binary diffusivities of i and j $m^2\ s^{-1}$
$D_{i,j}^{eff}$	effective binary diffusivities of i and j $m^2\ s^{-1}$
D	diffusivity of oxygen in ionomer $m^2\ s^{-1}$
D_{eff}	effective diffusivity of oxygen in ionomer $m^2\ s^{-1}$
D_p	particle diameter
F	Faraday's constant C mol^{-1}
f	overlapping ratio
H	Henry's constant atm $m^3\ mol^{-1}$
I_v^{CL}	current generation per unit volume of CL A m^{-3}
i_0^{ref}	reference exchange current density A cm^{-2}
M_n	molecular weight of gas mixture kg mol^{-1}
M_j	molecular weight of species j kg mol^{-1}
m	number of contact points
m_{Pt}	Pt loading mg cm^{-2}
NFP	Nafion weight ratio
n	number of agglomerate per unit volume of CL
P	pressure atm
P_{O_2}	oxygen partial pressure atm
P_{H_2}	hydrogen partial pressure atm
$Pt\|C$	platinum carbon weight ratio
R	gas constant mol $cm^{-2}\ s^{-1}$
R_{O_2}	volumetric oxygen reaction rate mol $m^{-3}\ s^{-1}$
R_{HO_2}	volumetric reaction rate for water vapor mol $m^{-3}\ s^{-1}$
r_{agg}	agglomerate radius m
r_{Pt}	Pt particle radius m
T	temperature K
Th	Thiele modulus
t_{cl}	catalyst layer thickness m
α_c	charge transfer coefficient
α_m	packing factor
α_{OD}	electroosmotic drag coefficient
δ	ionomer film thickness m
ε_{GDL}	porosity of GDL
$\varepsilon_{V,cr}$	critical porosity
$\varepsilon_{V,o}$	limiting porosity
ε_v	porosity of CL
ε_{agg}	ionomer volume fraction in agglomerate
ρ	density kg m^{-3}
σ_s	electron conductivity S m^{-1}
σ_s^{eff}	effective electron conductivity S m^{-1}
σ_m	ionic conductivity S m^{-1}
σ_m^{eff}	effective ionic conductivity S m^{-1}
ϕ_s	electron potential V
ϕ_m	ionic potential V
ϕ_{RH}	local relative humidity
ω_i	mass fraction of species i

References

[1] F.C. Cetinbas, S.G. Advani, A.K. Prasad, J. Electrochem. Soc. 161 (6) (2014).
[2] M. Uchida, Y. Aoyama, N. Eda, A. Ohta, J. Electrochem. Soc. 142 (12) (1995).
[3] E. Antolini, L. Giorgi, A. Pozio, E. Passalacqua, J. Power Sources 77 (1999).
[4] V.A. Paganin, E.A. Ticinalli, E.R. Gonzalez, J. Appl. Electrochem. 26 (1996).
[5] E. Passalacqua, F. Lufrano, G. Squadrito, A. Patti, L. Giorgi, Electrochim. Acta 46 (2001).
[6] Z. Qi, A. Kaufman, J. Power Sources 113 (2003).
[7] E.A. Ticianelli, J.G. Beery, S.J. Srinivasan, Appl. Electrochem. 21 (1991).
[8] E.A. Ticianelli, C.R. Derouin, S.J. Srinivasan, Electroanal. Chem. 251 (1988).
[9] O. Antoine, Y. Butel, P. Ozil, R. Burand, Electrochim. Acta 45 (2000).
[10] D.P. Wilkinson, J. St-Pierre, J. Power Sources 113 (2003).
[11] Z. Xie, R. Chow, K. Shi, T. Navessin, Q. Wang, D. Song, B. Andreaus, M. Eikerling, Z. Liu, S. Holdcroft, J. Electrochem. Soc. 152 (6) (2005).
[12] Q. Wang, M. Eikerling, D. Song, Z. Liu, T. Navessin, Z. Xie, S. Holdcroft, J. Electrochem. Soc. 151 (7) (2004).
[13] W. Sun, B.A. Peppley, K. Karana, Electrochim. Acta 50 (2005).
[14] D. Song, Q. Wang, Z. Liu, M. Eikerling, Z. Xie, T. Navessin, S. Holdcroft, Electrochim. Acta 50 (2005).
[15] D.H. Schwarz, N. Djilali, Int. J. Energy Res. 33 (2009).
[16] M. Srinivasarao, D. Bhattacharyya, R. Rengaswamy, S. Narasimhan, Int. J. Hydrogen Energy 35 (2010).
[17] P.P. Mukherjee, C.-Y. Wang, J. Electrochem. Soc. 154 (11) (2007).
[18] F.C. Cetinbas, S.G. Advani, A.K. Prasad, J. Power Sources 250 (2014).
[19] F.C. Cetinbas, S.G. Advani, A.K. Prasad, J. Electrochem. Soc. 160 (8) (2013).